This article has been accepted for publication in a future issue of this journal, but has not been fully edited. Content may change prior to final publication. Citation information: DOI 10.1109/TMAG.2015.2434614, IEEE Transactions on Magnetics

Strain-Induced High Coercivity in $La_{0.7}Sr_{0.3}CoO_3$ Films

Y. Y. Zhao, H.W. Yang, Y. Liu, H. Kuang, M. Zhang, W. L. Zuo, J. Wang, F. X. Hu*, J. R. Sun, and B. G. Shen

Beijing National Laboratory for Condensed Matter Physics and State Key Laboratory of Magnetism, Institute of Physics, Chinese Academy of Sciences, Beijing 100190

Here, we report strain-induced high coercivity in $La_{0.7}Sr_{0.3}CoO_3$ (LSCO) films, which suffer in-plane tensile strains due to the positive lattice mismatch between the substrate and the LSCO bulk. The films on (011)-PMN-PT exhibit large uniaxial anisotropy, large coercivity and high saturation magnetization at low temperature in contrast to the well soft magnetic behaviors in LSCO bulk. It is found that the coercivity of the 40 nm (001)-LSCO/STO film can be as high as 1.45 T at 10K and the observed coercivity decreases rapidly as the thickness increases, though the curie temperature is below room temperature. The large coercivity and anisotropy should be closely related to the strain-induced structural changes and the different orbital ordering of Co^{3+} and Co^{4+} ions. Meanwhile, the enhanced domain wall pinning by the tensile strain may also contribute to the observed high coercivity.

***Index Terms*—high coercivity, non-rare-earth permanent magnets, spin, strain effect**

I. Introduction

The development of new permanent magnet materials is of particularly importance since the high-performance $Nd_2Fe_{14}B$ are expensive due to the limited reserves of rare earth Nd, Tb, Dy on the earth [1], [2]. In the past several years, much attention has been attracted to the permanent magnet without rare earth [3], [4], such as Zr_2Co_{11}, $HfCo_7$ and Mn-based alloys, and excellent performance has been observed. For example, the achieved energy products can be as high as 19.5 MGOe in Zr_2Co_{11}: Fe-Co nano-composites film. The permanent magnetic films are mainly used in micromotor and microwave isolator/circulator. The substrates are usually insulating or semiconductive materials while the conventional permanent magnetic films are mainly metallic materials. There are two main hindrances that cannot be avoided during film preparation. (i) The lattice mismatch introduced by the difference between the bulk and substrates. In previous studies, metallic buffer layer was introduced to overcome the lattice mismatch, which is a good way to prevent film dropping off. However, the films deposited by this method are mainly non-oriented polycrystalline which makes their easy axes distribute randomly and is disadvantageous to the performance of the permanent magnet. (ii) The metallic films can be easily oxidized. This problem can be overcome partially by a cap layer [5]. Thus, three layers are usually needed to compose the permanent magnetic films, which make the preparation process more complex. Till now, the two hindrances mentioned above are still unsolved despite many efforts are made. The well inoxidability makes the magnetic oxide film a potential candidate for high performance permanent magnetic film. Ferrite magnetic films were considered firstly. However, investigations show that the saturation magnetization and coercivity of this kind of films are much lower than that of the metallic permanent magnetic films, which is a serious disadvantage.

Previous studies revealed that the magnetic and electronic properties of $La_{1-x}Sr_xCoO_3$ systems can be influenced easily by the interplay between the spin-state degree of freedom. In the ground state, the parent compound $LaCoO_3$ (LCO) is a typical Mott insulators, showing nonmagnetim under a low-spin (LS). With increasing the temperature, the Co^{3+} ions can be thermally excited to an intermediate spin (IS) state when the temperature above 35 K, and a mixed state of IS and high spin (HS) above 300 K. Furthermore, a HS state appears in the LCO system above 550 K accompanied with a metal-insulator transition [6]. By doping LCO with divalent ion Sr, the systems would transfer into ferromagnetic for x>0.18. It is generally believed that replacing La^{3+} by Sr^{2+} creates Co^{4+}, which increases the ferromagnetic double exchange interaction (DE) between Co^{4+} and Co^{3+}. However, researches revealed that the FM metallic state of the bulk $La_{1-x}Sr_xCoO_3$ appears mostly below room temperature, which is disadvantageous to possible potential application. Recently, studies [7], [8] show that the external factor (high pressure, lattice strain) can also adjust the spin-state. Similarly, a strain-induced enhancement of the FM state was also observed in both LCO and $LaSrCoO_3$ films [6], [9], [10]. However, a further investigation of the strain-dependent magnetic properties in $La_{1-x}Sr_xCoO_3$ films is still lacking. In this paper, we report strain-induced high coercivity in the Co-based $La_{0.7}Sr_{0.3}CoO_3$ (LSCO) films.

II. EXPERIMENTAL

LSCO targets were prepared by conventional solid phase sintering method. The commercial purities of starting powders La_2O_3, $SrCO_3$, and Co_3O_4 are 99.99, 99.99, and 99.7 wt.%, respectively. To introduce different strains, two kinds of substrates with different lattice constants and orientations, (001)-$SrTiO_3$ (STO, 3.905 Å), (011)-0.7Pb$(Mg_{1/3}Nb_{2/3})O_3$-0.3$PbTiO_3$(PMN-PT, 4.017 Å), were chosen to deposit LSCO thin films with various thickness using PLD technique. A KrF excimer laser with a wavelength of 248 nm and a repetition rate of 2 Hz was used. During the deposition, the substrate temperature was 730 ℃ and the background oxygen pressure was kept at 50 Pa. After the deposition, the films were cooled down to room temperature in 100 Pa oxygen atmosphere to compensating the oxygen deficiency. The thickness of films

Manuscript received January 1, 2008
Corresponding author: F. X. Hu (e-mail: fxhu@iphy.ac.cn).
Digital Object Identifier inserted by IEEE

0018-9464 (c) 2015 IEEE. Personal use is permitted, but republication/redistribution requires IEEE permission. See http://www.ieee.org/publications_standards/publications/rights/index.html for more information.

This article has been accepted for publication in a future issue of this journal, but has not been fully edited. Content may change prior to final publication. Citation information: DOI 10.1109/TMAG.2015.2434614, IEEE Transactions on Magnetics

was controlled to be 30, 40 and 100 nm, respectively. The crystalline structure of the LSCO bulk and films has been measured using X-ray diffraction (XRD) with Cu-Kα radiation. Magnetic properties were measured by a superconducting quantum interference device-vibrating sample magnetometers (SQUID–VSM).

III. RESULTS AND DISCUSSION

X-ray diffraction (XRD) measurements indicated that the bulk LSCO displays orthorhombic structure with *Pnma* space group and all films are grown with high texture crystallinity. Fig. 1 displays a typical XRD pattern for the 40 nm LSCO film on STO substrate. It demonstrates that the film is highly oriented along the [001] direction and no other impurity phases and textures were found. From the XRD pattern, the

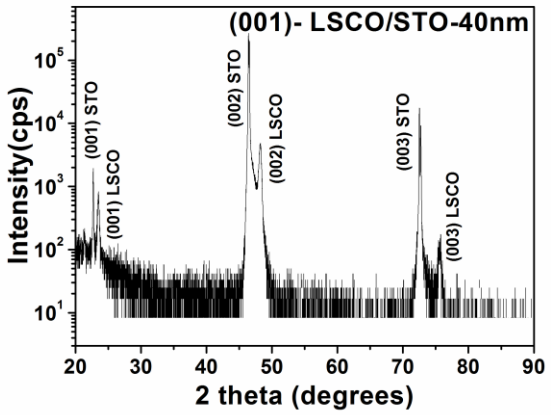

Fig.1. X-ray diffraction patterns of 40 nm LSCO film on STO substrate

lattice parameters are determined as c~3.766 Å and a~3.861 Å, assuming the volume of the unit cell retains the same as that of the bulk under stress. The in-plane strain is calculated as 1.08% by using the equation of $\varepsilon_{xx}=(a_f-a_b)/a_b$, where a_f is the lattice parameter of the film and a_b is the lattice parameter of the bulk. It's obvious that the film experiences in-plane tensile strain, which is consistent with the lattice mismatch between the bulk LSCO (a~3.82 Å) and the substrate of STO (a~3.905 Å). The full information of all films' lattice parameters and estimated lattice strains are listed in Table I. One can find that the estimated in-plane tensile strain for the film on STO reduces from 1.13% for the 30 nm LSCO film to 0.79% for the 100 nm film, indicating a gradual strain relaxation with increasing the film thickness. However, the 40 nm film on PMN-PT experiences a smaller in-plane tensile strain (0.54%) along [100] direction compared to either 30 nm or 100 nm film on STO despite the PMN-PT substrate has a larger lattice mismatch with the LSCO material than STO. This fact suggests that a few lattice defects exist in the film on PMN-PT due to the probably incoherent growth of the film [10].

Fig. 2(a) displays the temperature dependent magnetization (M-T) measured under 0.05 T using zero-field cooling (ZFC) and field cooling (FC) for LSCO bulk. It can been found that the long range ferromagnetic ordering appears at low temperature, and the Curie temperature (T_C) is about 224 K

Table I. Summary of thickness, out-of-plane lattice constants, a-axis lattice constants and in-plane strains for LSCO film on various substrates.

	thickness	a_{sub} (Å)	out-of-plane lattice constants (Å)	a_{film}-(100) (Å)	In-plane strain
(001)LSCO/STO	30	3.905	3.764 [001]	3.863	1.13%[100]
	40	3.905	3.766 [001]	3.861	1.08%[100]
	100	3.905	3.788 [001]	3.850	0.79%[100]
(011)LSCO/PMN-PT	40	4.017	2.692 [011]	3.841	0.54%[100] 0.56%[01-1]
Bulk	Lattice parameter: 3.82 Å				

which is consistent with previous reports[11], [12]. A distinct separation between the ZFC and FC curves appears below the transition temperature, which may be attributed to a spin-glass state caused by the gradual block of the moments of the ferromagnetic clusters with decreasing temperature. The M-T curves for LSCO/STO films with different thickness are shown in Fig. 2(b). The Curie temperature T_C are determined, from the M-T curves, to be 173 K, 185 K and 219 K for 30 nm, 40 nm and 100 nm films, respectively. One can find that the T_C deviates significantly from the bulk value (224 K) and decreases with reducing the film thickness, which may partially owe to the size effect. As well known, the size effect can shift the T_C to lower temperatures when the spin–spin correlation length exceeds the film thickness [13]. Meanwhile,

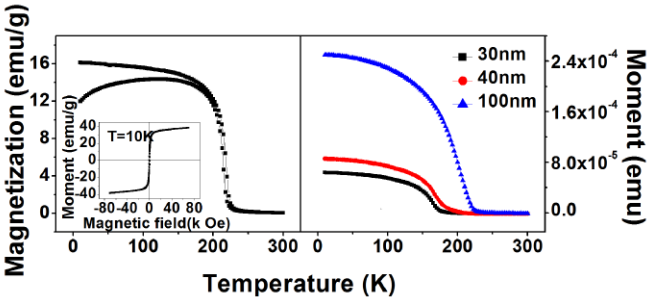

Fig. 2. The temperature-dependent magnetization (M-T) of LSCO bulk and films measured under 0.05 T field. a) LSCO bulk in both ZFC and FC process, inset: the magnetic hysteresis loops of bulk recorded at 10 K. b) the M-T curves for LSCO/STO films with different thickness.

the in-plane tensile strain introduced from the substrate may also play an important role in affecting the T_C. The in-plane tensile strain tends to reduce the Co–O bond overlap, resulting in a decreasing of the critical temperature of the double-exchange interaction. Furthermore, the variation of the Co-O bond length would violate the delicate balance between the crystal splitting and the intra-atomic Hund exchange coupling, leading to the transition of spin state among low spin (LS), intermediate spin (IS) and high spin (HS) and thus the T_C. The magnetic hysteresis loops (M-H) of bulk recorded at 10K was also presented in the inset of Fig 2(a). Similar to previous investigations, the LSCO bulk does not show hard magnetic properties but displays good soft magnetic behaviors with coercivity approaching zero [14]. However, for the strained-films, a quite different ferromagnetic (FM) behavior is

0018-9464 (c) 2015 IEEE. Personal use is permitted, but republication/redistribution requires IEEE permission. See http://www.ieee.org/publications_standards/publications/rights/index.html for more information.

This article has been accepted for publication in a future issue of this journal, but has not been fully edited. Content may change prior to final publication. Citation information: DOI 10.1109/TMAG.2015.2434614, IEEE Transactions on Magnetics

identified from the M-H curves.

Fig.3 (a) shows the magnetic hysteresis loops (M-H) of 40nm LSCO films on (011)-PMN-PT measured at 10 K. The magnetic field up to 5 T is applied along the in-plane [100] and [01-1] directions, respectively. Firstly, one can notice that the film displays significant anisotropic M-H loops along the in-plane [100], [01-1] directions. The perfect squareness of M-H loops along the in-plane [01-1] direction indicates that the [01-1] is the easy-axis while the [100] is the hard-axis. The coercivity is about 0.56 T for the [01-1] direction. Such high coercivity and large uniaxial anisotropy indicate that the in-plane tensile strained-film behaves some hard magnetism, different from the bulk LSCO. Meanwhile, the maximum magnetization measured along easy-axis and hard-axis are almost the same, which indicates that the sample has been magnetized to the saturated state under 5 T magnetic field. The saturation magnetization is about 71 emu/g, which is almost twice the value of bulk LSCO. The tensile strain can enlarge the in-plane lattice parameter and lead to a tetragonal distortion in the LSCO film, which results in further reduction of the separation between the upper t_{2g} and lower e_g levels. Thus, more intermediate spin (IS) or high spin (HS) state in Co ions may be induced by the tensile strain, resulting in a high saturation magnetization.

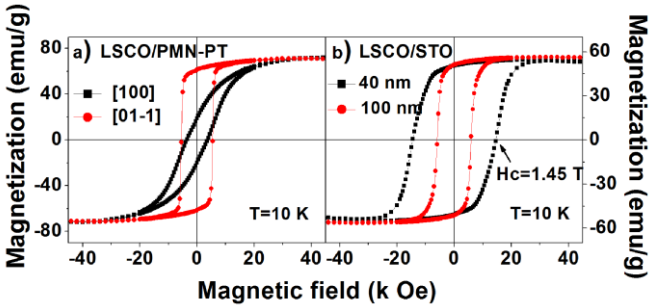

Fig.3. The magnetic hysteresis (M-H) loops measured at 10 K for the LSCO films. a) 40 nm (011)-LSCO/PMN-PT for in-plane [100] and [01-1] directions. b) 40 nm and 100 nm (001)-LSCO/STO films

The M-H loops of 40 nm and 100nm (001)-LSCO/STO films measured at 10 K with magnetic field along the in-plane [100] direction are displayed in Fig. 3(b). One can surprisingly find that the coercivity of the thinner film can be as high as 1.45 T. As the film thickness increases to 100 nm, the introduced tensile strain from the substrate is partially relaxed (Table I) and the coercivity reduces to 0.6 T while the squareness and remanent magnetization keep nearly unchanged. Similarly, by comparing the properties of 40 nm films on different substrates PMN-PT and STO, one can find that the coercivity of LSCO/PMN-PT film along [01-1] easy-axis is 0.56 T, which is smaller than 1.45 T of LSCO/STO film, noting the tensile strain of former is smaller than that of the latter by half. All these observed coercivity in the strained films are much larger than the one of bulk LSCO, indicating that the in-plane tensile strain plays a critical role in producing the high coercivity for the LSCO film. Furthermore, these results are consistent with the fact that the in-plane tensile strain in the 40 nm-LSCO/STO film is larger compared to that in the 100 nm film and the film on PMN-PT, demonstrating that the induced coercivity increases with the increase of in-plane tensile strain. Despite the exact reason of large coercivity induced by tensile strain in LSCO films is unclear at this moment, we may reveal a tip of the iceberg of the underlying principle by considering the correlations between magnetic and electric properties. The further investigations on the transport measurements demonstrate that all the films on both STO and PMN-PT display FM insulating behavior, in contrast to the metal FM behavior of the bulk. The tensile strain-induced Jahn-Teller-type distortion of the CoO_6 octahedra in the films may affect the orbital ordering of Co^{3+} and Co^{4+} ions, thus favoring the FM super-exchange interactions, similar to the case in the low-doped $La_{1-x}Ca_xMnO_3$ systems. The large coercivity and anisotropy should be closely related to the specific structural characteristics and the different orbital ordering of Co^{3+} and Co^{4+} ions caused by tensile strains. On the other hand, the introduced tensile strain may also induce an inhomogeneous distribution of FM domain [15], [16], resulting a pinning of domain wall and thus the extra contribution to high coercivity.

IV. Conclusion

In conclusion, we have successfully fabricated highly textured LSCO films on STO and PMN-PT substrates. The films suffer out-of-plane compressive strains and in-plane tensile strains due to the positive lattice mismatch between the substrate and the LSCO bulk. For all films, the T_C deviates significantly from the bulk value (224 K) and T_C decreases with reducing the film thickness, which may owe to the size and strain effect. The tensile strained films on (011)-PMN-PT exhibit large uniaxial anisotropy, large coercivity and high saturation magnetization, while the LSCO bulk shows good soft magnetic behaviors with coercivity approaching zero. Interestingly, the coercivity of the 40 nm LSCO/STO film can be as high as 1.45 T. All these observed high coercivity in the strained films are much larger than the one of bulk LSCO, indicating that the in-plane tensile strain plays a critical role in producing the high coercivity for the LSCO film. Furthermore, as the films become thicker, the observed coercivity decreases rapidly due to the relaxation of the in-plane tensile strain. The observed large coercivity and anisotropy in present strained LSCO film should be closely related to the tensile strain induced structural changes and the different orbital ordering of Co^{3+} and Co^{4+} ions. Meanwhile, the tensile strain may further introduce extra domain wall pinning and contribute to the observed high coercivity."

Acknowledgment

This work was supported by the National Basic Research Program of China (973 program, Grant Nos. 2014CB643702 and 2012CB933000), the National Natural Sciences Foundation of China (Grant Nos. 51271196, 11174345 and 11474341).

0018-9464 (c) 2015 IEEE. Personal use is permitted, but republication/redistribution requires IEEE permission. See http://www.ieee.org/publications_standards/publications/rights/index.html for more information.

This article has been accepted for publication in a future issue of this journal, but has not been fully edited. Content may change prior to final publication. Citation information: DOI 10.1109/TMAG.2015.2434614, IEEE Transactions on Magnetics

REFERENCES

[1] N. Jones, "The Pull of Stronger Magnets," *Nature*, vol. 472, no. 7341, pp. 22-23, Apr 7, 2011.

[2] J. M. D. Coey, "Permanent magnets: Plugging the gap," *Scripta Materialia*, vol. 67, no. 6, pp. 524-529, Sep, 2012.

[3] B. Balasubramanian, B. Das, R. Skomski, W. Y. Zhang, and D. J. Sellmyer, "Novel nanostructured rare-earth-free magnetic materials with high energy products," *Adv Mater*, vol. 25, no. 42, pp. 6090-3, Nov 13, 2013.

[4] G. V. Ivanova, N. N. Shchegoleva, and A. M. Gabay, "Crystal structure of Zr2Co11 hard magnetic compound," *Journal of Alloys and Compounds*, vol. 432, no. 1-2, pp. 135-141, 2007.

[5] M. Valetas, M. Vérité, A. Bessaudou, F. Cosset, and J. C. Vareille, "Rf-sputtering deposition and magnetic characterisation of Nd–Fe–B thin films for microwave applications," *Computational Materials Science*, vol. 33, no. 1-3, pp. 163-167, 2005.

[6] H. W. Yang, H. R. Zhang, Y. Li, S. F. Wang, X. Shen, Q. Q. Lan, S. Meng, R. C. Yu, B. G. Shen, and J. R. Sun, "Anomalous magnetism in strained $La_{(1-x)}Sr_{(x)}CoO_3$ epitaxial films ($0 \le x \le 0.5$)," *Sci Rep*, vol. 4, pp. 6206, 2014.

[7] Y. F. Lu, J. Klein, F. Herbstritt, J. B. Philipp, A. Marx, and R. Gross, "Effect of strain and tetragonal lattice distortions in doped perovskite manganites," *Physical Review B*, vol. 73, no. 18, May, 2006.

[8] M. Ziese, H. C. Semmelhack, and K. H. Han, "Strain-induced orbital ordering in thin $La_{0.7}Ca_{0.3}MnO_3$ films on $SrTiO_3$," *Physical Review B*, vol. 68, no. 13, Oct 1, 2003.

[9] R. Lengsdorf, M. Ait-Tahar, S. Saxena, M. Ellerby, D. Khomskii, H. Micklitz, T. Lorenz, and M. Abd-Elmeguid, "Pressure-induced insulating state in (La,Sr)CoO_3," *Physical Review B*, vol. 69, no. 14, 2004.

[10] A. Rata, A. Herklotz, K. Nenkov, L. Schultz, and K. Dörr, "Strain-Induced Insulator State and Giant Gauge Factor of $La_{0.7}Sr_{0.3}CoO_3$ Films," *Physical Review Letters*, vol. 100, no. 7, 2008.

[11] M. Kriener, C. Zobel, A. Reichl, J. Baier, M. Cwik, K. Berggold, H. Kierspel, O. Zabara, A. Freimuth, and T. Lorenz, "Structure, magnetization, and resistivity of $La_{1-x}M_xCoO_3$ (M=Ca, Sr, and Ba)," *Physical Review B*, vol. 69, no. 9, 2004.

[12] H. Aarbogh, J. Wu, L. Wang, H. Zheng, J. Mitchell, and C. Leighton, "Magnetic and electronic properties of $La_{1-x}Sr_xCoO_3$ single crystals across the percolation metal-insulator transition," *Physical Review B*, vol. 74, no. 13, 2006.

[13] M. Fisher, and M. Barber, "Scaling Theory for Finite-Size Effects in the Critical Region," *Physical Review Letters*, vol. 28, no. 23, pp. 1516-1519, 1972.

[14] M. A. Senaris-rodriguez, and J. B. Goodenough, "Magnetic and transport properties of the system $La_{1-x}Sr_xCoO_{3-\delta}$ ($0<x\le0.50$)" *Journal of Solid State Chemistry*, vol. 118, no. 2, pp. 323-336, Sep, 1995.

[15] Y. Y. Zhao, J. Wang, H. Kuang, F. X. Hu, H. R. Zhang, Y. Liu, Y. Zhang, S. H. Wang, R. R. Wu, M. Zhang, L. F. Bao, J. R. Sun, and B. G. Shen, "Abnormal percolative transport and colossal electroresistance induced by anisotropic strain in (011)-$Pr_{0.7}(Ca_{0.6}Sr_{0.4})_{0.3}MnO_3$/PMN-PT heterostructure," *Scientific Reports*, vol. 4, Nov 17, 2014.

[16] J. Dho, Y. N. Kim, Y. S. Hwang, J. C. Kim, and N. H. Hur, "Strain-induced magnetic stripe domains in $La_{0.7}Sr_{0.3}MnO3$ thin films," *Applied Physics Letters*, vol. 82, no. 9, pp. 1434-1436, Mar 3, 2003.

0018-9464 (c) 2015 IEEE. Personal use is permitted, but republication/redistribution requires IEEE permission. See http://www.ieee.org/publications_standards/publications/rights/index.html for more information.